

Try Depth Instead of Weight Correlations: Mean-field is a Less Restrictive Assumption For Deeper Networks

Sebastian Farquhar¹ Lewis Smith¹ Yarin Gal¹

Abstract

We challenge the longstanding assumption that the mean-field approximation for variational inference in Bayesian neural networks is severely restrictive. We argue mathematically that full-covariance approximations only improve the ELBO if they improve the expected log-likelihood. We further show that deeper mean-field networks are able to express predictive distributions approximately equivalent to shallower full-covariance networks. We validate these observations empirically, demonstrating that deeper models decrease the divergence between diagonal- and full-covariance Gaussian fits to the true posterior.

1. Introduction

While performing variational inference (VI) in Bayesian neural networks (BNNs) researchers often make the ‘mean-field’ approximation that weight distributions are independent (i.e., diagonal weight covariance) (Hinton & van Camp, 1993; Graves, 2011; Blundell et al., 2015).¹ Researchers have assumed that the mean-field approximation is a severe one ever since Barber & Bishop (1998) first framed the method in the language of variational inference and introduced full covariance between weights within a layer. Unfortunately, modelling the full covariance requires quadratically more parameters than the mean-field case, and comes with large computational costs. Because of the difficulties of full-covariance methods, and the presumed inadequacy of mean-field networks, researchers have invested significant effort into tractable structured covariance approximations (Louizos & Welling, 2016; Sun et al., 2017; Oh et al., 2019) or richer posterior families (Jaakkola & Jordan, 1998; Gershman et al., 2012; Mnih & Gregor, 2014; Rezende & Mohamed, 2015; Louizos & Welling, 2017; Sun et al.,

¹OATML Research Group, Department of Computer Science, University of Oxford. Correspondence to: Sebastian Farquhar <sebastian.farquhar@cs.ox.ac.uk>.

¹See Appendix A for a brief introduction to variational inference in Bayesian neural networks.

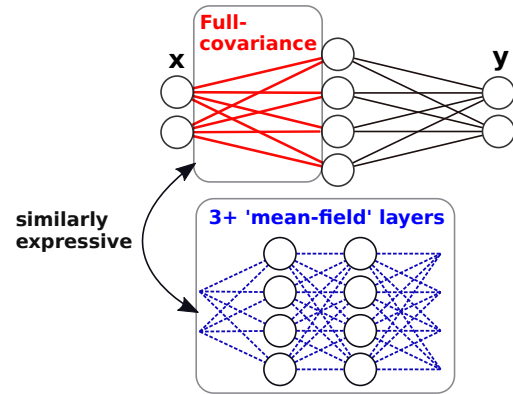


Figure 1. Three or more mean-field weight layers can approximate a full-covariance weight layer when doing so would improve the expected log-likelihood. So, in deeper models, an explicitly full-covariance weight posterior may not be needed.

2019).

We challenge the presumed inadequacy of mean-field distributions for deep BNNs: in deeper models the mean-field approximation becomes less restrictive.

We argue theoretically, in §2, that covariance between the *weights* of the approximate posterior will hurt the evidence-lower-bound loss unless it improves the expected log-likelihood *function*. But deeper neural networks with mean-field weight distributions can be approximately as expressive as shallower full-covariance ones in this regard. We also show that an arbitrarily large neural network with a mean-field weight distribution can approximate any non-zero predictive distribution on a continuous domain (we later consider networks which are not arbitrarily large).

In order to bridge the analysis of the function- and weight-space, in §3 we examine a deep network without non-linear activations. In the linear case, we can collapse L weight matrices through matrix multiplication into a single *product matrix*, whose distribution is identifiable with a distribution over linear functions. We show that for $L \geq 3$, the resulting product matrix can have non-zero covariance entries everywhere. This means that a deeper linear mean-field network can induce a similar distribution in function space as a shallower full-covariance network (see Figure 1). In §4 we

extend this result to deep neural networks with piecewise-linear activations, like ReLUs, by showing that for any given input we can construct the *product matrix of a linearized function* in the neighbourhood of the input which shows similar behaviour.

We test this empirically in §5. We visualize the product matrix of a linearized function and show that it locally corresponds with the linear case. Moreover, we show that the distribution of entries in a product matrix composed of mean-field Gaussian distributions can be multi-modal, addressing a commonly held objection to Gaussian approximating distributions. We examine the similarity between a diagonal- and full-covariance Gaussian approximation to the true posterior (measured as a KL-divergence) and show that the approximations become more similar as models get deeper. Lastly we show, in a simple setting where full-covariance VI is tractable, that mean-field VI matches full-covariance VI’s expected log-likelihood as the depth grows. That is, the price we pay for the mean-field approximation is lower in deeper models.

Our work has three main implications for future research. First, it motivates renewed exploration into resolutions of other problems with mean-field VI, like gradient variance. Second, future work that introduces more complicated posteriors will need to ensure that the cost of the extra expressiveness is lower than the cost of using a deeper model. Third, it emphasises the importance of Bayesian deep learning performance benchmarks that include deeper models, rather than those that typically use a single layer of hidden units like the widely-used UCI experimental settings.

2. Why Do We Want Full Covariance?

It is instructive to consider why we are interested in a full-covariance approximate posterior in the first place. Barber & Bishop (1998) point out that the KL between an approximate posterior, $q(\theta)$, and a true posterior which has off-diagonal covariance entries, $p(\theta|\mathcal{D})$, is tighter if the approximate posterior can also express off-diagonal covariance (see Figure 2).

In our work, we first develop a more detailed understanding by considering a different view of the $KL(q(\theta) \parallel p(\theta|\mathcal{D}))$ above—the evidence-lower-bound (ELBO) which is optimized in VI—before considering the posterior predictive distribution ($p(y|\mathbf{x}, \mathcal{D})$) directly.

2.1. Full Covariance Helps and Hurts the ELBO

The ELBO differs from the KL to the posterior only by the log marginal likelihood, which is constant. Optimizing the ELBO is therefore equivalent to optimizing the KL to the posterior. The ELBO can be written as the difference between the expected log-likelihood of the data and the KL-

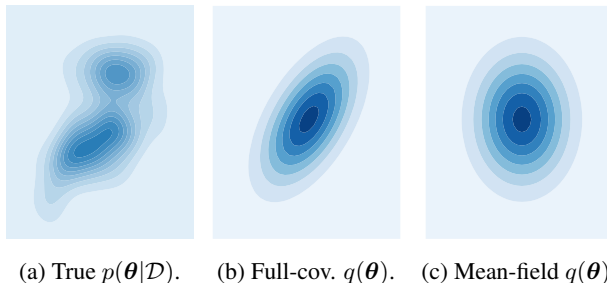


Figure 2. (a) A hypothetical weight posterior with covariance between weights could be fit more closely by an approximate posterior (b) with full-covariance than (c) one with a mean-field weight distribution. This reasoning has historically motivated full-covariance approximate posteriors (Barber & Bishop, 1998).

divergence between the approximate posterior and the *prior*:

$$\mathbb{E} [\log(p(y|\theta, \mathbf{x}))] - KL(q(\theta) \parallel p(\theta)). \quad (1)$$

Typically when using a multivariate Gaussian prior for a neural network we should use a diagonal prior covariance: it is not that we have a prior belief that the weights are uncorrelated, but rather that we have no reason to think any two non-identical weights are more likely to be positively or negatively correlated a priori. By symmetry, our prior should therefore put zero correlation between any two non-identical weights. If a hierarchical prior is used, the expectation of the covariance between non-identical weights should be zero. The KL-divergence term in the ELBO therefore puts pressure on the approximate posterior to have diagonal covariance because the approximate posterior distribution which minimizes this term must have diagonal covariance.

This establishes a tension with the expected log-likelihood term. The log-likelihood is maximized when the probability of the actual measurement is high, under the model. A model which expresses covariance between weights might help express functions which can maximize that expected log-likelihood.

Examining the ELBO therefore shows that unless covariance lets your distribution over functions predict the data better it will not improve your ELBO. The increase in the KL to the prior which is caused by off-diagonal covariance must be offset by a bigger improvement in the log-likelihood of the data. This is only possible if the full-covariance approximate posterior is able to represent a distribution which has a better expected log-likelihood and there exists no diagonal-covariance approximate posterior which can give the same improvement in expected log-likelihood.

What we show below, however, is that several mean-field layers can, together, express ‘product layers’ with off-diagonal correlations. This means that an approximate posterior with explicitly full-covariance layers might buy little improve-

ment to the functional expressiveness of the posterior for *deep* networks. As a result, unless we have prior reasons to expect particular structures of posterior covariance, we should feel free to use the mean-field approximation in deep networks. Note, however, that this is not necessarily an argument for switching to a deeper model—switching changes the probabilistic model in which we do inference and may affect the KL term. Rather, we argue that once one is already using a relatively deep model, the gain from an explicit covariance may be small because the network is able to learn where/if it is useful to approximate full-covariance.

This argument is particularly suited to VI because of its mode-seeking behaviour. In a large, over-parameterized model there is flexibility for at least one of the modes of the posterior to be approximated by a mean-field distribution with good log-likelihood and KL to the prior. Under a mode-covering approach such as expectation propagation the approximate posterior would be forced to cover approximately diagonal modes as well as ones that require a full-covariance approximating distribution.

2.2. Approximating Arbitrary Predictive Distributions

We might worry that a neural network with a mean-field distribution over its weights cannot represent some posterior predictive functions. This concern was raised in Foong et al. (2019), who argue that a single-layer network with a mean-field approximate posterior cannot learn ‘in-between’ uncertainty—to be appropriately uncertain in an unexplored region between two regions of input space that are present in the training data.

But, as they acknowledge, this need not be a problem for deeper networks. We can extend an argument of Gal (2016) to show that any predictive distribution on a continuous input domain, $p(y|\mathbf{x})$, that is non-zero on any open set can be approximated arbitrarily closely by a neural network with a mean-field distribution over the weights. A special case of a mean-field distribution is a deterministic one, which allows us to use universal approximation theorems (Hornik et al., 1989).²

Construct a neural network with a mean-field distribution over the weights in two parts. The first part is a neural network expressing some distribution over its output hidden units $p(\mathbf{h}|\mathbf{x}, \boldsymbol{\theta})$ with mean-field weights $\boldsymbol{\theta}$, and can be a single layer. The second part is a deterministic neural network that takes \mathbf{h} as inputs and induces a distribution $p(y|\mathbf{x}, \boldsymbol{\theta})$. The weights of this deterministic transformation are distributed with a delta function and are therefore independent

²Foong et al. (2019) show a slightly weaker result, that a 2+ layer BNN with a mean-field distribution can express a continuous predictive function with any mean and variance. They also use the universal approximation theorem, but require a more contrived network structure.

of each other.³

We want to find a BNN such that marginalizing over the weights results in an arbitrary predictive distribution. To do so, we find a continuous mapping from the distribution over \mathbf{h} to a uniform distribution⁴, and then the inverse cumulative density function (c.d.f.) of the target predictive distribution⁵ $p(y|\mathbf{x})$. This would map the distribution over \mathbf{h} onto the target distribution. If such a mapping exists (though it need not be analytically expressible), we can use the second part of the network to approximate the mapping arbitrarily closely, using the universal approximation theorem. Marginalizing over this entire BNN (both the stochastic and deterministic parts) therefore gives the target distribution. This lets a neural network with a mean-field weight distribution express any non-zero predictive distribution with a continuous input domain, without needing any covariance between weights.

Unfortunately, this hypothetical network might have a very bad ELBO. In order to get the delta functions required for the universal approximation theorem we must change the prior to be infinitesimally tight, and the resulting ELBO would suffer. Nevertheless, we show empirically in §5 that mean-field approximate posteriors are able to reach similar log-likelihoods to full-covariance ones without appealing to arbitrarily large networks.

In the next sections, we return to a weight-space perspective and consider some ways in which deep networks with mean-field approximate posteriors can simulate shallower full-covariance ones.

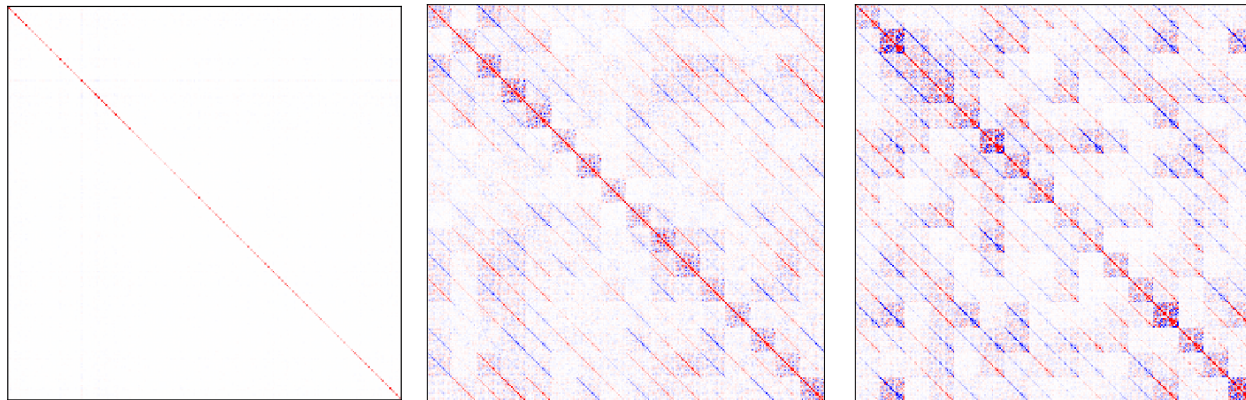
3. Emergence of Full Covariance in Deep Linear Networks

We are most interested in neural networks that have non-linear activations. However, we can gain considerable analytical insight from the study of linear neural networks, which we investigate in §3.1 and §3.2. The key observation for our linear analysis is that L weight matrices for a neural network without non-linear activations can be ‘flattened’ through matrix multiplication into a single weight matrix—the distribution of weights in this product matrix is identifiable with a distribution over linear functions. In §3.2, we prove that for $L \geq 3$ the resulting product matrix can have non-zero covariance between every element. We show that in practice, at different depths, it is able to learn a variety of complicated covariance structures. Later, in

³Alternatively, we can instead consider a diagonal multivariate Gaussian whose variance becomes arbitrarily small. In the limit, the universal approximation theorems will apply.

⁴This is just the c.d.f. of \mathbf{h} . For a neural network with mean-field Gaussian weight distributions this exists, though it is not analytically expressible.

⁵This c.d.f exists and is invertible if the target predictive is strictly monotonic and continuous.



(a) Single weight matrix.

(b) 5-layer product matrix.

(c) 10-layer product matrix.

Figure 3. Covariance heatmap for linear ‘neural networks’. In a deep linear model we can examine the *product matrix* composed of L mean-field weight matrices. Here we show the covariance matrices from L -layer product matrices of networks trained on FashionMNIST. Redder is more positive, bluer more negative. (a) For one weight matrix, covariance is mean-field so only the diagonal entries non-zero. (b,c) For deeper models, the mean-field layers induce full-covariance product matrices with differing structures.

§4 we extend this analysis to non-linear activations before testing our predictions empirically in §5.

3.1. Simple Illustration and Visualization

To develop our intuitions, let us consider a linear model with a 2×2 weight matrix, W , with two input features and two outputs. We can choose to reparameterize the weight matrix as the product of two matrices, A and B . This corresponds to a neural network with a single layer of hidden units, but without a non-linear activation. We can write down the values of the elements of the product matrix in terms of the elements of A and B :

$$\mathbf{y} = W\mathbf{x} = B\mathbf{A}\mathbf{x} \quad (2)$$

$$= \begin{pmatrix} b_{11} & b_{12} \\ b_{21} & b_{22} \end{pmatrix} \begin{pmatrix} a_{11} & a_{12} \\ a_{21} & a_{22} \end{pmatrix} \mathbf{x} \quad (3)$$

$$= \begin{pmatrix} b_{11}a_{11} + b_{12}a_{21} & b_{11}a_{12} + b_{12}a_{22} \\ b_{21}a_{11} + b_{22}a_{21} & b_{21}a_{12} + b_{22}a_{22} \end{pmatrix} \mathbf{x} \quad (4)$$

Suppose we make the mean-field approximation for each layer, so each weight in A and B is correlated only with itself. Despite that, the resulting covariance matrix of W is not diagonal because elements share the same random variables. For example, b_{11} , highlighted in red, is in each entry in the top row, so elements of the top row have non-zero covariance with each other. We can create a product matrix with non-diagonal covariance by stacking mean-field layers.

In Figure 3 we visualize the covariance between entries of the product matrix from a trained mean-field VI linear model. Even though each weight matrix makes the mean-field assumption, the product develops off-diagonal correlations. The experiment is described in more detail in §5.1.

3.2. Non-zero Entries for Product Matrix Covariance

Using a recursive derivation for the covariance between elements of the product matrix we show that *only three* weight matrices (two layers of hidden units) are enough for non-zero covariance between all elements of the product matrix. The derivations in this section do not assume distributional family of the weights (e.g., not necessarily Gaussian), but do assume finite first and second moments.

Consider a similar setting as in §3.1, except that we allow ourselves K units in the hidden layer. We will use index notation to simplify the algebra, and consider the product matrix, $M^{(L)}$, which is the matrix product of an arbitrary mean-field weight matrix, $W^{(L)}$, and the product matrix with one fewer layers, $M^{(L-1)}$:

$$m_{ab}^{(L)} = \sum_{i=1}^K w_{ai}^{(L)} m_{ib}^{(L-1)}. \quad (5)$$

Here we set aside bias parameters, as they complicate the algebra, but adding them only strengthens the result because each bias term affects an entire row.

This allows us to frame the question: for what number of layers, L , is the covariance of the elements of the product matrix $\text{Cov}(m_{ab}^{(L)}, m_{cd}^{(L)})$ non-zero everywhere?

Lemma 1. *For $L \geq 3$ the product matrix covariance may be non-zero everywhere.*

Proof Sketch. We explicitly derive the covariance between elements of the product matrix and show that for $L = 3$ all entries in the covariance matrix are non-zero so long as the entries of W have non-zero means. The recursion shows that once an $M^{(L)}$ has non-zero covariance between each element, then $M^{(L')}$ for all $L' \geq L$ also has non-zero

covariance between each element (except for perversely constructed weight distributions). The full derivation can be found in Appendix C.1. \square

This means that, in the linear case at least, for $L \geq 3$ (two layers of hidden units) we can recover a product matrix with non-zero covariance between all weights even if each individual layer is mean-field. As a result, a sequence of mean-field layers induces a product matrix that could approximate a full-covariance layer.

This does not guarantee that arbitrary covariances can be approximated. For example, a mean-field model simply has fewer parameters than a full-covariance model of the same depth. This places a bound on the minimum number of mean-field layers needed to have enough free variables to even possibly fit a full-covariance layer exactly.⁶ Also note that the distribution over entries of the product of Gaussian weight matrices is not in general Gaussian. See Appendix C.2 for further exploration of the product matrix distribution and demonstration that weight priors can be chosen that approximately maintain the same product matrix prior regardless of depth. In §5 we offer empirical evidence that the mean-field and full-covariance distributions do in practice become more similar with depth.

4. Extending to Non-linear Activations

Neural networks use non-linear activations to increase the flexibility of function approximation. On the face of it, these non-linearities make it impossible to consider product matrices.

In this section we show how to define the *product matrix of a linearized function*, which is an extension of the product matrix to widely used neural networks with piecewise-linear activation functions like ReLUs or Leaky ReLUs. For this we draw inspiration from a proof technique by Shamir et al. (2019) which we extend to the stochastic matrices case. Neural networks with piecewise-linear activations are themselves piecewise-linear. These piecewise-linear neural networks define hyperplanes which partition the input domain into regions within which the neural network is a linear function. Each region can be identified by a sign vector that indicates which activations are ‘switched on’.

We show in Appendix C.3.1 that the piecewise-linearity of the neural network means that for any input point \mathbf{x}^* (almost

⁶Suppose we have Gaussian weights parameterized by mean and variance. A product matrix of L mean-field layers has $L * 2 * K^2$ parameters. Meanwhile a single full-covariance weight matrix would have had K^2 mean parameters and K^4 covariance parameters.

anywhere w.r.t. a Lebesgue measure⁷), there is a non-zero-measure region around that point where the neural network function f_{θ} is linear. This lets us construct a product matrix within that region using a locally linear realizations of the network weights, θ_i . Since f_{θ_i} is linear in that region, we can compute a product matrix $M_i^{(L)}$ corresponding to that function realization and input. We overcome the fact that different realizations of f_{θ_i} can have different sign vectors by defining a random variate, for a given \mathbf{x}^* , over the elements of the product matrix constructed in this way by sampling realizations θ_i and applying the sign vector appropriate to each one. The product matrix of a linearized function can be found empirically, and resembles the product matrices from linear settings (see Figure 4).

Using this random variate, we derive a similar result to lemma 1 for the product matrix of a linearized function, extending §3 to non-linear neural networks. We prove in Appendix C.3 that, similarly to the linear case, covariance between elements of this product matrix of a linearized function can be non-zero in general. The exception, which depends on the data, is when the input happens to be in a part of space where almost all the activations are zero. However, if the data is remotely near the training distribution this should never happen in a trained model. Because the precise values of the covariance become data-dependent, which makes analytical results difficult beyond identifying that non-zero off-diagonal covariance is possible.

5. Empirical Evaluation

We empirically validate our theoretical analysis. First, we calculate the product matrix of a linearized function from a deep mean-field neural network trained on the FashionMNIST dataset, and show that it demonstrates the expected off-diagonal behaviours, as well as noting it can express a multi-modal posterior. Second, we examine diagonal- and full-covariance Gaussian fits to samples from the true posterior distribution (sampled using ‘gold-standard’ Hamiltonian Monte Carlo), and show that the divergence between the two Gaussian distributions becomes tighter as the model becomes deeper. This result is particularly strong because it models full covariance between *all* weights in the model, not just those that share a layer as in Barber & Bishop (1998). Last, we show that the difference in log-likelihood between full- and diagonal-covariance approximate posteriors falls as depth increases, on a small dataset.

5.1. The Product Matrix of Linearized Functions

We validate the product matrix of a linearized function construction empirically using a neural network trained with

⁷The zero-measure exception being where the input lies precisely on an inflection point of the ReLU network.

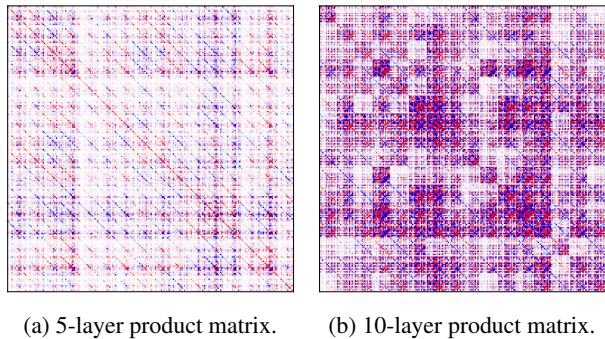


Figure 4. Covariance matrix between entries of the product matrix of a linearized Leaky ReLU BNN trained on FashionMNIST. Like the linear case, depth allows stronger off-diagonal correlations. The activation patterns introduce extra correlation between weights that share rows.

Leaky ReLU activations with $\alpha = 0.1$. We calculate the product matrix of a linearized function for a randomly chosen test example from the FashionMNIST dataset, using an L -layer multi-layer perceptron with a width of 16 units trained on FashionMNIST. Each sample of the product matrix is calculated by taking a realization of the weights, calculating the activation pattern on the test example (same example each time), multiplying the activation pattern into each weight matrix, and doing the full matrix multiplication. This allows us to estimate the covariance between entries of the product matrix of the linearized function, in a manner analogous to the linear visualization in Figure 3.

The heatmap of the covariance matrix between entries in the resulting product matrix of a linearized function is shown in Figure 4. Just like in the linear case, as the model gets deeper the induced distribution on the product matrix shows complex off-diagonal covariance. The presence of activations induces additional correlations between weights that share a row. This demonstrates that neural networks with piecewise-linear activations can use multiple layers to emulate a single full-covariance layer, which might allow deep networks to improve the log-likelihood without explicitly modelling covariance. See Appendix B.1 for further experimental details.⁸

Further, since researchers often critique a Gaussian approximate posterior because it is unimodal, we confirm empirically that multiple mean-field layers can induce a multimodal product matrix distribution. In Figure 5 we show a density over an element of the product matrix of a linearized function from three layers of weights in a Leaky ReLU BNN with $\alpha = 0.1$. The induced distribution is multi-modal. We

⁸We observe the interesting phenomenon that the covariance matrices based on trained linear models seem to have a block structure. However we did not observe a block structure in randomly sampled covariance matrices shown in the appendix.

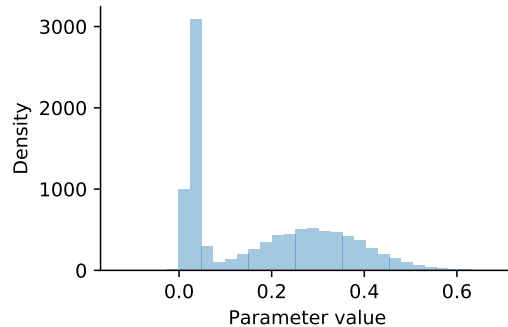


Figure 5. The product matrix of a linearized function also allows the unimodal Gaussian layers to approximate multimodal distributions over product matrix entries. Here, we show an example density over a product matrix element, from a three-layer Leaky ReLU model with mean-field Gaussian distributions over each weight trained on FashionMNIST.

visually examined the distributions over 20 randomly chosen entries of this product matrix and found that 12 were multi-modal. We found that without the non-linear activation, none of the product matrix entry distributions examined were multimodal, suggesting that the non-linearities in fact play an important role in inducing rich predictive distributions by creating modes corresponding to activated sign patterns.

5.2. Difference Between Full- and Diagonal-covariance Fit to ‘True’ Posterior

We show that the ‘price’ of the mean-field approximation falls as we increase the depth of a neural network. That is to say, the best Gaussian fit to the true posterior with full-covariance between all weights anywhere in the model becomes increasingly similar to the diagonal-covariance fit as the model becomes deeper. We use the ‘gold-standard’ posterior approximation technique, Hamiltonian Monte Carlo (HMC), in order to avoid the optimization challenges of deep full-covariance neural networks. HMC also allows us to express a truly full-covariance posterior, not even assuming that layers are independent of each other, unlike Barber & Bishop (1998) and most structured covariance approximations.

At a high level, we assess similarity using the KL divergence between a diagonal Gaussian fit to the true posterior and a full-covariance Gaussian fit— $KL(q_{\text{diag}}(\theta) \parallel q_{\text{full}}(\theta))$. We show in Figure 6 that the divergence between these distributions falls as the model becomes deeper. Moreover, the KL falls both for linear and non-linear neural networks. We can interpret this KL divergence as the worst case information loss, measured in nats, caused by using the diagonal approximation to the full-covariance approximate poste-

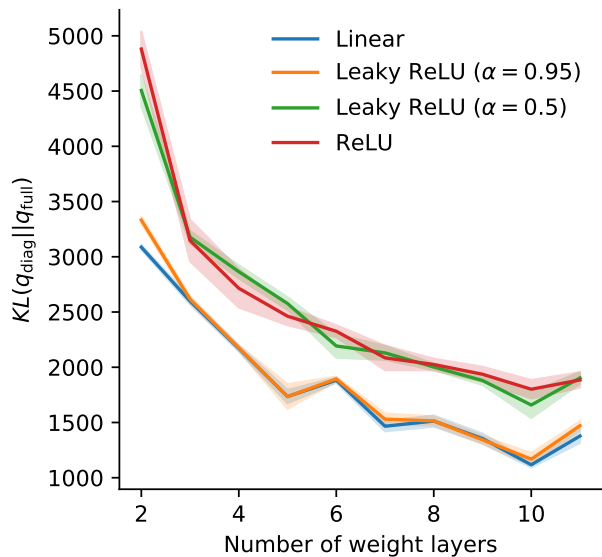


Figure 6. The mean-field approx. posterior becomes more similar to the full-covariance one as the model gets deeper, measured by KL divergence. This means that the ‘price’ we pay for the mean-field approximation falls as the model becomes deeper. All models have roughly 1,000 parameters. Shading is s.e. of mean.

rior.⁹ Although the KL does not fall to zero, note that nats correspond to exponentially many representable states, so more-than-halving the KL is a huge reduction in lost information.

All models have roughly the same number of parameters (1,000), regardless of depth, and are trained on the 2-dimensional binary classification task ‘two moons’.¹⁰ We can interpolate between the linear and ReLU networks by using Leaky ReLU networks with different values of α , showing that the behaviour of the diagonal covariance is more a matter of degree in the scaling of α than whether the network has non-linearities at all, which supports the applicability of the analysis of §3.

There is some nuance in the estimation of the Gaussian fit to the true posterior. We begin with HMC using No U-turn Sampling (Hoffman & Gelman, 2014). A naive approach would simply be to fit the samples from HMC using a Gaussian distribution. However, when we examined the samples, we found that the posterior was sometimes multimodal, so a naive Gaussian would be spread between multiple modes (see Figure 7). We address this by fitting a

⁹For a discrete probability distribution, the KL divergence would be the amount of information gained by using the full-covariance approximate posterior rather than the diagonal-covariance. In our continuous case, it is the supremum of this information gain under any discretization (Gray, 2011).

¹⁰From scikit-learn’s datasets.make_moons, with 500 training points and noise parameter 0.1.

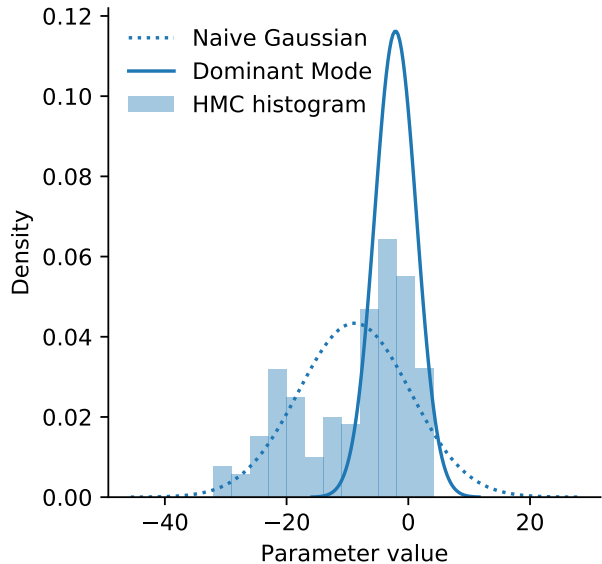


Figure 7. Example density for randomly chosen parameter from a ReLU network with three hidden layers. The HMC histogram is multimodal. If we picked the naive Gaussian fit, we would lie between the modes. By using a mixture model, we select the dominant mode, for which the Gaussian is a better fit.

Gaussian mixture model to the HMC samples and using the most highly weighted component of the mixture distribution as the Gaussian fit (‘dominant mode’ in Figure 7). We optimize the number of components in the mixture using the Bayesian information criterion. Note that we are only trying to establish how costly the *mean-field* approximation is, not how costly the *Gaussian* approximation is. There may well still be weaknesses in using a Gaussian approximation to the posterior, our argument is just that we do not gain much by explicitly modelling full covariance.

In order to find the diagonal-covariance Gaussian fit, we find the diagonal distribution that minimizes $KL(q_{\text{diag}}(\theta) \parallel q_{\text{full}}(\theta))$. This can be analytically calculated (see Appendix B.2, where we also discuss hyperparameters and implementation of the experiments in this section).

5.3. Effect of Depth on Log-likelihood in Full- and Diagonal-covariance Networks

We compare the effect of depth on the performance of full- and diagonal-covariance neural networks. In Figure 8, we show the test cross-entropy of models of varying depths on the Iris dataset from the UCI repository. As one might expect, for a single layer of hidden units (two layers of weights) a full-covariance posterior is able to achieve a lower cross-entropy. As the depth increases, however, the cross-entropy of the mean-field network matches the full-covariance one (and exceeds it, though this is simply an optimization issue as the space of full-covariance distribu-

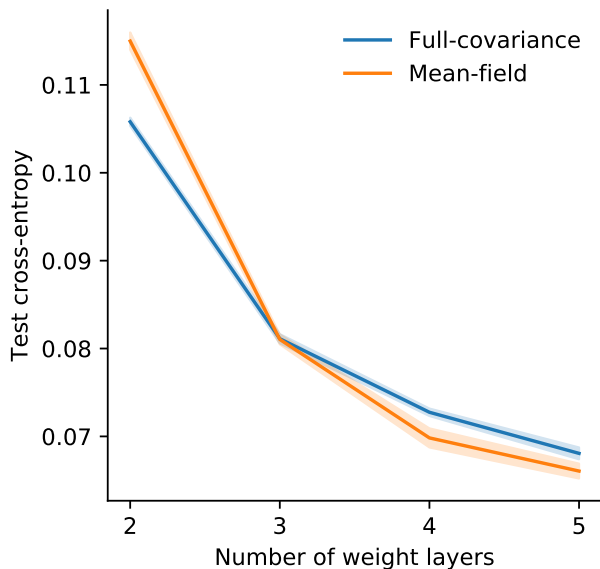


Figure 8. The full-covariance approximate posterior reaches a lower log-likelihood (cross-entropy in classification setting) than the mean-field approximation for two weight layers (single hidden unit layer). But for deeper models the mean-field approximation matches the full-covariance.

tions includes the space of mean-field ones). Full details of the experiment can be found in Appendix B.3.

6. Prior Work

It has generally been assumed that the mean-field approximation, while important for tractable inference, is too restrictive. Recent work has identified pathologies in single-layer mean-field VI (Foong et al., 2019) while earlier work has suggested its limitations in time-series models (Turner & Sahani, 2011). Extensive research has sought to avoid its limitations by introducing full or structured approximations to the covariance (Barber & Bishop, 1998; Louizos & Welling, 2016; Sun et al., 2017; Oh et al., 2019); by modelling a richer approximate posterior (Jaakkola & Jordan, 1998; Mnih & Gregor, 2014; Rezende & Mohamed, 2015; Louizos & Welling, 2017); or by performing VI directly on the function (Sun et al., 2019). Despite widespread assertions that the mean-field approximation results in a problematically restricted approximate posterior in deep neural networks, there has been no work *in deep neural networks* demonstrating this.

Meanwhile, other researchers have identified and corrected problems with mean-field VI that have nothing to do with the restrictiveness of the mean-field approximation, but rather to do with gradient variance (Wu et al., 2019; Farquhar et al., 2020).

7. Consequences and Discussion

We have shown, in §2, that a full covariance posterior over neural network weights only helps the ELBO if it improves the data log-likelihood. However, in *deep* neural networks, full-covariance approximate posteriors do little to help express distributions over functions that could not be expressed with mean-field approximate posteriors. Moreover, we showed that a neural network with a mean-field distribution over weights can, in principle, approximate any predictive distribution.

In §3 we argued that, in the linear setting, a stack of three or more mean-field weight matrices can approximate a single full-covariance weight matrix, and that we might therefore expect that at least some modes of deep neural network’s true posteriors will have nearly diagonal covariance. In §4 we argued that this analysis extends to neural networks with non-linear activations, and in §5 we show that this is borne out by empirical examinations.

Our work challenges the previously unchallenged assumption that mean-field VI fails because the posterior approximation is too restrictive. This increases the importance of investigating other causes of mean-field VI’s failures and fixing them, such as Wu et al. (2019) and Farquhar et al. (2020), and calls for research that builds more flexible posterior approximations to justify whether this flexibility helps in a deep learning setting. Last, our work is a reminder of the importance of testing Bayesian deep learning methods on benchmarks that use deep models, such as Filos et al. (2019), rather than the predominantly single-layer models used on the popular UCI benchmark.

Our work is a special case of a more general observation. The ability of an approximate posterior to fit a true posterior depends on the properties of the true posterior, which in turn depend on the model and data. We should therefore not think only about whether an approximate posterior is good or bad, but whether it is a good match to the model. The true posterior in a shallow neural network might have strong off-diagonal correlations, but the true posterior of a deep network may well have at least one mode that is nearly mean-field. With depth, we allow a rich posterior over predictive functions to come from a simple approximate posterior over each weight.

8. Acknowledgements

The authors would like to thank for their comments and conversations Wendelin Boehmer, Adam Cobb, Gregory Farquhar, Raza Habib, Clare Lyle, Michael Hutchinson, Sebastian Ober, and Hippolyt Ritter. We would especially like to thank Adam Cobb for his help applying the Hamiltorch package (Cobb et al., 2019).

This work was supported by the EPSCRC CDTs for Cyber Security and for Autonomous Intelligent Machines and Systems at the University of Oxford. It was also supported by the Alan Turing Institute.

References

- Barber, D. and Bishop, C. M. Ensemble Learning in Bayesian Neural Networks. In *Neural Networks and Machine Learning*, pp. 215–237. Springer, 1998. [1](#), [2](#), [5](#), [5.2](#), [6](#), [A](#)
- Blundell, C., Cornebise, J., Kavukcuoglu, K., and Wierstra, D. Weight Uncertainty in Neural Networks. *Proceedings of the 32nd International Conference on Machine Learning*, 37:1613–1622, 2015. [1](#)
- Bondesson, L. A Class of Probability Distributions that is Closed with Respect to Addition as Well as Multiplication of Independent Random Variables. *Journal of Theoretical Probability*, 28(3):1063–1081, September 2015. [C.2](#)
- Cobb, A. D., Baydin, A. G., Markham, A., and Roberts, S. J. Introducing an Explicit Symplectic Integration Scheme for Riemannian Manifold Hamiltonian Monte Carlo. *arXiv*, October 2019. arXiv: 1910.06243. [8](#), [B.2](#)
- Farquhar, S., Osborne, M., and Gal, Y. Radial Bayesian Neural Networks: Robust Variational Inference In Big Models. *Proceedings of the 23rd International Conference on Artificial Intelligence and Statistics*, 2020. [6](#), [7](#)
- Filos, A., Farquhar, S., Gomez, A. N., Rudner, T. G. J., Kenton, Z., Smith, L., Alizadeh, M., de Kroon, A., and Gal, Y. Benchmarking Bayesian Deep Learning with Diabetic Retinopathy Diagnosis. *Bayesian Deep Learning Workshop at NeurIPS*, 2019. [7](#)
- Foong, A. Y. K., Burt, D. R., Li, Y., and Turner, R. E. Pathologies of Factorised Gaussian and MC Dropout Posteriors in Bayesian Neural Networks. *Bayesian Deep Learning Workshop at NeurIPS*, September 2019. arXiv: 1909.00719. [2.2](#), [2](#), [6](#)
- Gal, Y. Uncertainty in Deep Learning. *PhD Thesis*, 2016. [2.2](#)
- Gershman, S. J., Hoffman, M. D., and Blei, D. M. Nonparametric Variational Inference. *International Conference on Machine Learning*, 2012. [1](#)
- Graves, A. Practical Variational Inference for Neural Networks. *Neural Information Processing Systems*, 2011. [1](#)
- Gray, R. M. *Entropy and Information Theory*. Springer US, 2 edition, 2011. ISBN 978-1-4419-7969-8. doi: 10.1007/978-1-4419-7970-4. [9](#)
- He, K., Zhang, X., Ren, S., and Sun, J. Deep Residual Learning for Image Recognition. *CVPR*, 7(3):171–180, 2016. [B.3](#)

- Hinton, G. and van Camp, D. Keeping Neural Networks Simple by Minimizing the Description Length of the Weights. *Proceedings of the 6th Annual ACM Conference on Computational Learning Theory*, 1993. 1
- Hoffman, M. D. and Gelman, A. The No-U-Turn Sampler: Adaptively Setting Path Lengths in Hamiltonian Monte Carlo. *Journal of Machine Learning Research*, 15:1593–1623, 2014. 5.2
- Hornik, K., Stinchcombe, M., and White, H. Multilayer feedforward networks are universal approximators. *Neural Networks*, 2(5):359–366, 1989. 2.2
- Jaakkola, T. S. and Jordan, M. I. Improving the Mean Field Approximation Via the Use of Mixture Distributions. In Jordan, M. I. (ed.), *Learning in Graphical Models*, NATO ASI Series, pp. 163–173. Springer Netherlands, Dordrecht, 1998. doi: 10.1007/978-94-011-5014-9_6. 1, 6
- Louizos, C. and Welling, M. Structured and Efficient Variational Deep Learning with Matrix Gaussian Posteriors. *International Conference on Machine Learning*, pp. 1708–1716, 2016. 1, 6
- Louizos, C. and Welling, M. Multiplicative Normalizing Flows for Variational Bayesian Neural Networks. In *International Conference on Machine Learning*, pp. 2218–2227, July 2017. 1, 6
- MacKay, D. J. C. A Practical Bayesian Framework for Backpropagation Networks. *Neural Computation*, 4(3): 448–472, 1992. A
- Mnih, A. and Gregor, K. Neural Variational Inference and Learning in Belief Networks. *International Conference on Machine Learning*, June 2014. 1, 6
- Oh, C., Adamczewski, K., and Park, M. Radial and Directional Posteriors for Bayesian Neural Networks. *Bayesian Deep Learning Workshop at NeurIPS*, February 2019. arXiv: 1902.02603. 1, 6
- Polya, G. *Mathematics and Plausible Reasoning*. Princeton University Press, 1954. 12
- Reddi, S. J., Kale, S., and Kumar, S. On the Convergence of Adam and Beyond. *International Conference on Learning Representations*, February 2018. B.3
- Rezende, D. J. and Mohamed, S. Variational Inference with Normalizing Flows. *International Conference on Machine Learning*, 2015. 1, 6
- Shamir, A., Safran, I., Ronen, E., and Dunkelman, O. A Simple Explanation for the Existence of Adversarial Examples with Small Hamming Distance. *arXiv*, January 2019. arXiv: 1901.10861. 4
- Springer, M. D. and Thompson, W. E. The Distribution of Products of Beta, Gamma and Gaussian Random Variables. *SIAM Journal on Applied Mathematics*, 18(4): 721–737, 1970. ISSN 0036-1399. C.2
- Sun, S., Chen, C., and Carin, L. Learning Structured Weight Uncertainty in Bayesian Neural Networks. *Artificial Intelligence and Statistics*, pp. 1283–1292, 2017. 1, 6
- Sun, S., Zhang, G., Shi, J., and Grosse, R. Functional variational Bayesian Neural Networks. *International Conference on Learning Representations*, 2019. 1, 6
- Turner, R. E. and Sahani, M. Two problems with variational expectation maximisation for time series models. In Barber, D., Cemgil, A. T., and Chiappa, S. (eds.), *Bayesian Time Series Models*, pp. 104–124. Cambridge University Press, Cambridge, 2011. ISBN 978-0-511-98467-9. doi: 10.1017/CBO9780511984679.006. 6
- Wu, A., Nowozin, S., Meeds, E., Turner, R. E., Hernandez-Lobato, J. M., and Gaunt, A. L. Deterministic Variational Inference for Robust Bayesian Neural Networks. *International Conference on Learning Representations*, 2019. 6, 7
- Xiao, H., Rasul, K., and Vollgraf, R. Fashion-MNIST: a Novel Image Dataset for Benchmarking Machine Learning Algorithms. *arXiv*, August 2017. B.1

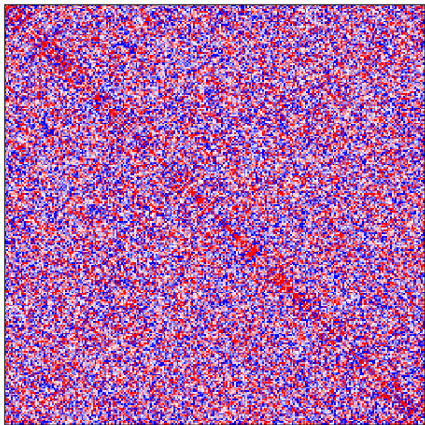


Figure 9. Unlike the covariance matrices of product matrix entries in models trained on real data, a randomly sampled product matrix does not show obvious block structure, though the noise makes it hard to be sure. This model has 5 linear layers.

A. Introduction to Variational Inference in Bayesian Neural Networks

A Bayesian neural network (BNN) places a distribution over the weights of a neural network (MacKay, 1992). We hope to infer the posterior distribution over the weights given the data. Because this is intractable, we seek an approximate posterior. Variational inference (VI) is one method for estimating that approximate posterior, in which we pick an approximating distribution and minimize the KL-divergence between it and the true posterior. For the full-covariance Gaussian approximate posterior (Barber & Bishop, 1998), the model weights for each layer θ_i are distributed according to the multivariate Gaussian distribution $\mathcal{N}(\mu_i, \Sigma_i)$. This is already a slight approximation, as it assumes layers are independent of each other. This is important for our analysis in §3 and §4, though note that the experiment in §5.2 does not assume any independence between layers.

The mean-field approximation restricts Σ_i to be a diagonal covariance matrix, or equivalently assumes that the probability distribution can be expressed as a product of individual weight distributions:

$$\mathcal{N}(\mu_i, \Sigma_i) = \prod_j \mathcal{N}(\mu_{ij}, \sigma_{ij}). \quad (6)$$

The MF approximation greatly reduces the computational cost of both forward and backwards propagation, and reduces the number of parameters required to store the model from order n^2 in the number of weights to order n .

B. Experimental Details

B.1. Full Description of Covariance Visualization

In §3.1 we consider the linear case, and in §4 we consider a Leaky ReLU non-linear activation with $\alpha = 0.1$.

In both cases we train a deep network on the Fashion MNIST dataset (Xiao et al., 2017). The network has L layers each with 16 hidden units. As a result the central portion of the model—everything except the first and last layers—is a sequence of 16x16 matrices. To illustrate, in the case of 2 layers of hidden units, the central portion is a single mean-field 16x16 weight matrix. For 11 layers of hidden units, there is a sequence of 10 mean-field matrices.

In the linear case, we can straightforwardly multiply realizations of these matrices and then numerically compute the covariance of the elements of the product matrix (we use 10,000 samples). In the non-linear case, we select a random test-datapoint and use it as \mathbf{x}^* as described in §4. We then calculate the activation patterns and adjust the individual weight layers given the actual activation patterns for each realization of the model at that point. We then calculate the covariance between product matrix elements as before.

In both cases the networks are trained using mean-field VI. We optimize with the Amsgrad variant of Adam with a learning rate of 0.001 and otherwise standard pytorch hyperparameters and batch size 64. We use 16 samples from the approximate posterior per batch. We use diagonal Gaussians as a prior, with mean zero and standard deviation 0.23 (see Figure 10 for motivation of this choice). We pretrain the means of the network with a single epoch with log-likelihood loss and then train for 9 further epochs with the full ELBO loss. The variance is parameterized using a softplus transformation initialized with $\rho = -3$. The dataset is preprocessed by normalizing mean and variance to (0,1) and with the last 10% of datapoints withheld for validation.

We compare these learned product matrices, in Figure 9, to a randomly sampled product matrix, to help understand which aspects of the product matrix’s covariance structure comes from the matrix multiplication as opposed to coming from the data. To do so, we sample weight layers whose entries are distributed normally. Each weight is sampled with standard deviation 0.3 and with a mean 0.01 and each weight matrix is 16x16. This visualization is with a linear product matrix of 5 layers. Unlike the experimental heatmaps, this randomly generated one does not show overt block structure, suggesting it might be a learned feature (though the heatmap is noisy enough that block structure is hard to determine).

B.2. HMC Experimental Settings

We begin by sampling from the true posterior using HMC.

We use the simple two-dimensional binary classification

‘make moons’ task using ¹¹. We use 500 training points (generated using `random_state = 0`). Using Cobb et al. (2019), we sample 1,000 times from the posterior given this data. We take 100 leapfrog steps per sample with an initial step size of 0.01, optimized using NUTS on 100 burn-in steps targeting a rejection rate of 0.8. We use a prior precision, normalizing constant, and τ of 1.0. The model is designed to have as close to 1000 non-bias parameters each time as possible, adjusting the width given the depth of the model.

Using these samples, we find a Gaussian fit. For each model we fit a Gaussian mixture model with between 1 and 4 components and pick the one with the best Bayesian information criterion (this was most often a 2-component model). We then find the best diagonal fit to this distribution, which is a Gaussian distribution with the same mean and with a precision matrix equal to the inverse of the diagonal precision of the full-covariance Gaussian.

Finally, we calculate the KL divergence between these two distributions. For each result, we recalculate the HMC samples 20 times. The graph reports the mean and shading reflects the standard error of the mean. All experiments in this and other sections were run on a desktop workstation with an Nvidia 1080 GPU.

B.3. Effect of Depth Measured on Iris Experimental Settings

We randomly split the Iris dataset into a training set of 100 datapoints and test set of 50 datapoints (details in code). We train models of varying depth with a width of four hidden units using either mean-field or full-covariance VI with a unit Gaussian prior. We use the Amsgrad variant of Adam (Reddi et al., 2018) with a learning rate of 10^{-3} . The mean-field and full-covariance means are initialized with a uniform He initialization (He et al., 2016). The mean-field variances are initialized with `softplus(-6) + 10-6`. The full-covariance covariances are initialized to an identity matrix scaled by 10^{-6} . Models are trained for up to 1000 epochs, or until the loss has not improved for 30 epochs. Unfortunately, for deeper models the initializations resulted in failed training for some seeds. To avoid this issue, we selected the 10 best seeds out of 100 training runs, and report the mean and standard error for these. Because we treat full- and diagonal-covariance in the same way, the resulting graph is a fair reflection of their relative best-case merits, but not intended as anything resembling a ‘real-world’ performance benchmark.

Readers may consider the Iris dataset to be unhelpfully

¹¹https://scikit-learn.org/stable/modules/generated/sklearn.datasets.make_moons.html#sklearn.datasets.make_moons

small, however this was a necessary choice. Optimizing a full-covariance approximate posterior is challenging because the correlation between weights introduces large gradient variance. As a result, we have used a network with only four hidden units per layer. In addition, the small number of training points creates a broad posterior, which is the best-case scenario for a full-covariance approximate posterior.

C. Proofs

C.1. Full Derivation of the Product Matrix Covariance

Consider a similar setting as in §3.1, except that we allow ourselves K units in the hidden layer. We will use index notation to simplify the algebra, and consider the product matrix, $M^{(L)}$, which is the matrix product of a mean-field weight matrix, $W^{(L)}$, and the product matrix with one fewer layers, $M^{(L-1)}$:

$$m_{ab}^{(N)} = \sum_{i=1}^K w_{ai}^{(N)} m_{ib}^{(N-1)}. \quad (7)$$

The weight matrix $W^{(L)}$ is assumed to have a mean-field distribution (the covariance matrix is zero for all off diagonal elements) with arbitrary means:

$$\text{Cov}(w_{ac}^{(L)}, w_{bd}^{(L)}) = \Sigma_{abcd}^{(L)} = \delta_{ac} \delta_{bd} \sigma_{ab}^{(L)}; \quad (8)$$

$$\mathbb{E} w_{ab}^{(L)} = \mu_{ab}^{(L)}. \quad (9)$$

Note that the weight matrix is 2-dimensional, but the covariance matrix is defined between every element of the weight matrix. While it can be helpful to regard it as 2-dimensional also, we index it with the four indices that define a pair of elements of the weight matrix.

We begin by deriving the expression for the covariance of the L -layer product matrix $\text{Cov}(m_{ab}^{(L)}, m_{cd}^{(L)})$.

First, we use the definition of the product matrix in equation (7):

$$\text{Cov}(m_{ab}^{(L)}, m_{cd}^{(L)}) = \text{Cov}\left(\sum_i w_{ai}^{(L)} m_{ib}^{(L-1)}, \sum_j w_{cj}^{(L)} m_{jd}^{(L-1)}\right). \quad (10)$$

We then simplify this using the linearity of covariance (for brevity call the covariance of the product matrix $\hat{\Sigma}_{abcd}^{(L)}$):

$$\hat{\Sigma}_{abcd}^{(L)} = \sum_{ij} \text{Cov}(w_{ai}^{(L)} m_{ib}^{(L-1)}, w_{cj}^{(L)} m_{jd}^{(L-1)}). \quad (11)$$

Next, we rewrite using the definition of covariance in terms

of a difference of expectations:

$$\hat{\Sigma}_{abcd}^{(L)} = \sum_{ij} \mathbb{E} [w_{ai}^{(L)} m_{ib}^{(L-1)} w_{cj}^{(L)} m_{jd}^{(L-1)}] - \mathbb{E} [w_{ai}^{(L)} m_{ib}^{(L-1)}] \mathbb{E} [w_{cj}^{(L)} m_{jd}^{(L-1)}]. \quad (12)$$

This can in turn be simplified using the fact that the new layer is independent of the previous product matrix:

$$\hat{\Sigma}_{abcd}^{(L)} = \sum_{ij} \mathbb{E} [w_{ai}^{(L)} w_{cj}^{(L)}] \mathbb{E} [m_{ib}^{(L-1)} m_{jd}^{(L-1)}] - \mathbb{E} [w_{ai}^{(L)}] \mathbb{E} [w_{cj}^{(L)}] \mathbb{E} [m_{ib}^{(L-1)}] \mathbb{E} [m_{jd}^{(L-1)}]. \quad (13)$$

We can now rewrite this in order to expose the dependence on the covariance of the smaller product matrix:

$$\begin{aligned} \hat{\Sigma}_{abcd}^{(L)} &= \sum_{ij} \left(\mathbb{E} [w_{ai}^{(L)} w_{cj}^{(L)}] - \mathbb{E} [w_{ai}^{(L)}] \mathbb{E} [w_{cj}^{(L)}] \right) \\ &\quad \cdot \left(\mathbb{E} [m_{ib}^{(L-1)} m_{jd}^{(L-1)}] - \mathbb{E} [m_{ib}^{(L-1)}] \mathbb{E} [m_{jd}^{(L-1)}] \right) \\ &\quad + \mathbb{E} [w_{ai}^{(L)}] \mathbb{E} [w_{cj}^{(L)}] \left(\mathbb{E} [m_{ib}^{(L-1)} m_{jd}^{(L-1)}] - \mathbb{E} [m_{ib}^{(L-1)}] \mathbb{E} [m_{jd}^{(L-1)}] \right) \\ &\quad + \mathbb{E} [m_{ib}^{(L-1)}] \mathbb{E} [m_{jd}^{(L-1)}] \left(\mathbb{E} [w_{ai}^{(L)} w_{cj}^{(L)}] - \mathbb{E} [w_{ai}^{(L)}] \mathbb{E} [w_{cj}^{(L)}] \right) \\ &= \sum_{ij} \text{Cov}(w_{ai}^{(L)}, w_{cj}^{(L)}) \cdot \text{Cov}(m_{ib}^{(L-1)}, m_{jd}^{(L-1)}) \\ &\quad + \mathbb{E} [w_{ai}^{(L)}] \mathbb{E} [w_{cj}^{(L)}] \text{Cov}(m_{ib}^{(L-1)}, m_{jd}^{(L-1)}) \\ &\quad + \mathbb{E} [m_{ib}^{(L-1)}] \mathbb{E} [m_{jd}^{(L-1)}] \text{Cov}(w_{ai}^{(L)}, w_{cj}^{(L)}). \end{aligned} \quad (14)$$

$$(15)$$

This gives us a recursive expression for the covariance of the product matrix.

It is straightforward to substitute in our expressions for mean and variance in a mean-field network provided in equation (8), where we use the fact that the initial $M^{(1)}$ product matrix is just a single mean-field layer.

In this way, we show that:

$$\begin{aligned} \hat{\Sigma}_{abcd}^{(2)} &= \sum_{ij} \left(\delta_{ac} \delta_{ij} \sigma_{ai}^{(2)} \right) \cdot \left(\delta_{ij} \delta_{bd} \sigma_{ib}^{(1)} \right) \\ &\quad + \mu_{ai}^{(2)} \mu_{cj}^{(2)} \left(\delta_{ij} \delta_{bd} \sigma_{ib}^{(1)} \right) \\ &\quad + \mathbb{E} [m_{ib}^{(1)}] \mathbb{E} [m_{jd}^{(1)}] \left(\delta_{ac} \delta_{ij} \sigma_{ai}^{(2)} \right) \end{aligned} \quad (16)$$

$$\begin{aligned} &= \sum_i \delta_{ac} \delta_{bd} \sigma_{ai}^{(2)} \sigma_{ib}^{(1)} \\ &\quad + \delta_{bd} \mu_{ai}^{(2)} \mu_{ci}^{(2)} \sigma_{ib}^{(1)} \\ &\quad + \delta_{ac} \mu_{ib}^{(1)} \mu_{id}^{(1)} \sigma_{ai}^{(2)}. \end{aligned} \quad (17)$$

The first term of equation (17) has the Kronecker deltas $\delta_{ac} \delta_{bd}$ meaning that it contains diagonal entries in the covariance matrix. The second term has only δ_{bd} meaning it contains entries for the covariance between weights that share a column. The third term has only δ_{ac} meaning it contains entries for the covariance between weights that share a row.

This covariance already has some off-diagonal terms, but it does not yet contain non-zero covariance for weights that share neither a row nor a column.

But we can repeat the process and find $\hat{\Sigma}_{abcd}^{(3)}$ using equation (15) and our expression for $\hat{\Sigma}_{ibjd}^{(2)}$:

$$\begin{aligned} \hat{\Sigma}_{abcd}^{(3)} &= \sum_{ij} \left(\delta_{ac} \delta_{ij} \sigma_{ai}^{(3)} \right) \cdot \hat{\Sigma}_{ibjd}^{(2)} \\ &\quad + \mu_{ai}^{(3)} \mu_{cj}^{(3)} \hat{\Sigma}_{ibjd}^{(2)} \\ &\quad + \mathbb{E} [m_{ib}^{(2)}] \mathbb{E} [m_{jd}^{(2)}] \left(\delta_{ac} \delta_{ij} \sigma_{ai}^{(3)} \right) \end{aligned} \quad (18)$$

$$\begin{aligned} &= \sum_{ij} \left(\delta_{ac} \delta_{ij} \sigma_{ai}^{(3)} \right) \cdot \sum_k \left(\delta_{ij} \delta_{bd} \sigma_{ik}^{(2)} \sigma_{kb}^{(1)} \right. \\ &\quad \left. + \delta_{bd} \mu_{ik}^{(2)} \mu_{jk}^{(2)} \sigma_{kb}^{(1)} \right. \\ &\quad \left. + \delta_{ij} \mu_{kb}^{(1)} \mu_{kd}^{(1)} \sigma_{ik}^{(2)} \right) \\ &\quad + \mu_{ai}^{(3)} \mu_{cj}^{(3)} \cdot \sum_k \left(\delta_{ij} \delta_{bd} \sigma_{ik}^{(2)} \sigma_{kb}^{(1)} \right. \\ &\quad \left. + \delta_{bd} \mu_{ik}^{(2)} \mu_{jk}^{(2)} \sigma_{kb}^{(1)} \right. \\ &\quad \left. + \delta_{ij} \mu_{kb}^{(1)} \mu_{kd}^{(1)} \sigma_{ik}^{(2)} \right) \end{aligned}$$

$$+ \mathbb{E} [m_{ib}^{(2)}] \mathbb{E} [m_{jd}^{(2)}] \left(\delta_{ac} \delta_{ij} \sigma_{ai}^{(3)} \right). \quad (19)$$

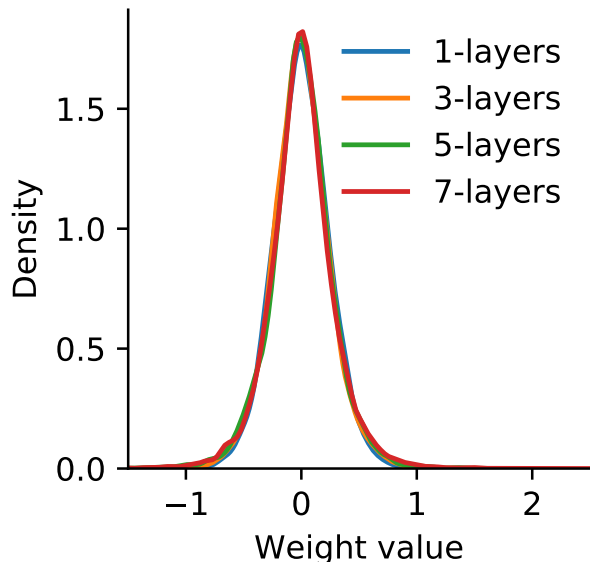


Figure 10. Density over arbitrary element of product matrix for L diagonal prior Gaussian weight matrices whose elements are i.i.d. $\mathcal{N}(0, 0.23^2)$. Product matrix elements are not strictly Gaussian, but very close.

It is the term in red which has no factors of Kronecker deltas in any of the indices a , b , c , or d . It is therefore present in all elements of the covariance matrix of the product matrix, regardless of whether they share one or both index. This shows that, so long as the distributional parameters themselves are non-zero, the product matrix can have a fully non-zero covariance matrix for $L = 3$. In addition, we observe that once the covariance of a product matrix is non-zero in some element, it can only become zero if the means of the weights are zero or the product of the means of the weights is equal to the covariance between all elements of a weight matrix (by inspection of equation (15)). This suffices to show that, except in exceptionally constructed circumstances, lemma 1 will hold.

C.2. Distribution of the Product Matrix

In general the distribution over the product of random variables is not the distribution over each of those variables. In the scalar case, the product of two independent Gaussian distributions is a generalized χ^2 distribution. The product of arbitrarily many Gaussians with arbitrary non-i.i.d. mean and variance is difficult to calculate (special cases are much better understood e.g., Springer & Thompson (1970)). An example of a distribution family that is closed under multiplication is the log-normal distribution.

In the case of matrix multiplication, important for neural network weights, because each element of a product of matrix multiplication is the sum of the product of individual

elements we would ideally like a distribution to be closed under both addition and multiplication (such as the Generalized Gamma convolution (Bondesson, 2015)) but these are not practical.

Instead, it would be helpful if we can ‘fudge’ things using the more helpful Gaussians but maintaining roughly similar distributions over product matrix elements as the network becomes deeper. For only one layer of hidden units, provided K is sufficiently large, we can use the central limit theorem to show that the elements of the product matrix composed of i.i.d. Gaussian priors tends to a Gaussian as the width of the hidden layer increases. For two or more layers, however, the central limit theorem fails because the elements of the product matrix are no longer independent. However, even though the resulting product matrix is not a Gaussian, we show through numerical simulation that products of matrices with individual weights distributed as $\mathcal{N}(0, 0.23^2)$ have roughly the same distribution over their weights. This, combined with the fact that our choice of Gaussian distributions over weights was somewhat arbitrary in the first place, might reassure us that the increase in depth does not change the model prior in an important way. In Figure 10 we plot the probability density function of an arbitrarily chosen entry in the product matrix with varying depths of diagonal Gaussian prior weights. The p.d.f. for 7 layers is approximately the same as the single-layer Gaussian distribution with variance 0.23^2 .

C.3. Proof of Linearized Product Matrix Covariance

C.3.1. PROOF OF LOCAL LINEARITY

We consider local linearity in the case of piecewise-linear activations like ReLU.

Lemma 2. *For almost any possible input point $\mathbf{x}^* \in \mathcal{D}$, for an input domain \mathcal{D} , for any realization of the model weights θ , the neural network function f_θ is linear in the neighbourhood of \mathbf{x}^* , and only a zero-measure set of points in \mathcal{D} do not fall in a region where f_θ is linear in a region with non-zero measure.*

Proof. Neural networks with finitely many piecewise-linear activations are themselves piecewise-linear. Therefore, for a finite neural network, we can decompose the input domain \mathcal{D} into regions $\mathcal{D}_i \subseteq \mathcal{D}$ such that

1. $\cup \mathcal{D}_i = \mathcal{D}$,
2. $\mathcal{D}_i \cap \mathcal{D}_j = \emptyset \quad \forall i \neq j$,
3. f_θ is a linear function on points in \mathcal{D}_i for each i .

Moreover, a neural network with m ReLU activations defines m hyperplanes dividing the input domain, which can

divide it into at most finitely many regions.¹² Except in the trivial case where the input domain has measure zero, this along with (1) and (2) jointly entail that at least one of the regions \mathcal{D}_i has non-zero measure. This, with (3) entails that only a set of input points of zero measure do *not* fall in a linear region of non-zero measure. These points correspond to inputs that lie directly on the inflection points of the ReLU activations. \square

C.3.2. DEFINING THE PRODUCT MATRIX OF A LINEARIZED FUNCTION

We define a random variate representing the product matrix of a linearized function, for an input point \mathbf{x}^* , using the following procedure. Take some input point \mathbf{x}^* . Sample a realization of the network weights, θ_i . Given lemma 2, the neural network f_{θ_i} linear in the neighbourhood of \mathbf{x}^* (except over a set of measure zero, in the case of activations like ReLU). If f_{θ_i} is linear, we can compute a product matrix $M_i^{(L)}$ corresponding to that function. For activations like ReLU and in the case \mathbf{x}^* corresponds exactly to an inflection point and the function is non-differentiable, we replace the function with the zero-function. This will only affect a set of input points of measure zero, so this is not important to implement in practice, but simplifies the analysis. We can define a random variate for elements of the product matrix constructed by sampling realizations θ_i . We denote the random variate representing the product matrix of a linearized function with P

C.3.3. PROOF THAT P HAS NON-ZERO OFF-DIAGONAL COVARIANCE

Theorem 1. *Given a mean-field distribution over the weights of f , in the neighbourhood of \mathbf{x}^* , f can be written in terms of the product matrix of a linearized function P . Elements of P can have non-zero off-diagonal covariance so long as $L \geq 3$.*

Proof. First, we show that the covariance between arbitrary entries of each realization of the product matrix of linearized functions can be non-zero. Afterwards, we will show that this implies that the covariance between arbitrary entries of the product matrix random variate, P can be non-zero.

Consider the case of an activation that is non-zero (almost everywhere). Then the derivation of lemma 1 proceeds trivially for each product matrix realization $M_i^{(L)}$, defined in the region around \mathbf{x}^* according to lemma 2. The derivation is only altered by a non-zero product over each row,

¹²Specifically: $\sum_{i=0}^{|\mathcal{D}|} \binom{m}{i}$ distinct regions (potentially fewer if some regions are empty) (Polya, 1954)). For piecewise-linear activations with more than one non-linear inflection point, the number of hyperplanes described in point (4) is correspondingly higher, but still finite.

reflecting the activation, but as this is non-zero the overall covariance is non-zero under the same conditions. This applies in the case of, for example, Leaky ReLUs.

Having established non-zero correlations are possible between arbitrary elements of $M_i^{(L)}$ for $L \geq 3$ we now need to show that this allows non-zero correlations between elements of P . The covariance of the sum of independent random variables is the sum of their covariances. Therefore the covariance of I realizations of P is:

$$\text{Cov}(P_{ab}, P_{cd}) = \frac{1}{I} \sum_{i=1}^I \text{Cov}(M_i^{(L)}_{ab}, M_i^{(L)}_{cd}). \quad (20)$$

The summands are, in general non-zero. We show by counter-example that the summands do not cancel out in general in our experiments in §5. This proves that it is possible to have non-zero covariance between entries of P .

Now consider the case of an activation that can be zero, like a ReLU. In order for it to be possible for the covariance between arbitrary elements of P to be non-zero we must show that a sufficiently large subset the summands are non-zero. In the case of ReLUs this is data-dependent. For some point in input space, the sign vector will have all activations switched off for all realizations of the model. For such a point, the network will effectively be a much shallower one which takes the final layer bias as inputs, and will not have any product matrix correlations. However, in practice it is very unlikely that a trained neural network will turn off all its activations for any typical input, nor that enough activations will be zero that the product matrix does not have shared elements after some depth. Because of the data-dependence, we cannot prove this analytically in general, although in the same way as the Leaky ReLU case we are able to show by example that non-zero correlations are possible between off-diagonal entries. \square